Light Field Projection for Lighting Reproduction

Zhong Zhou[1†] Tao Yu[1*] Xiaofeng Qiu[1] Ruigang Yang[2] Qinping Zhao[1]

[1]State Key Laboratory of Virtual Reality Technology and Systems
Beihang University

[2]Center for Visualization and Virtual Environments
University of Kentucky

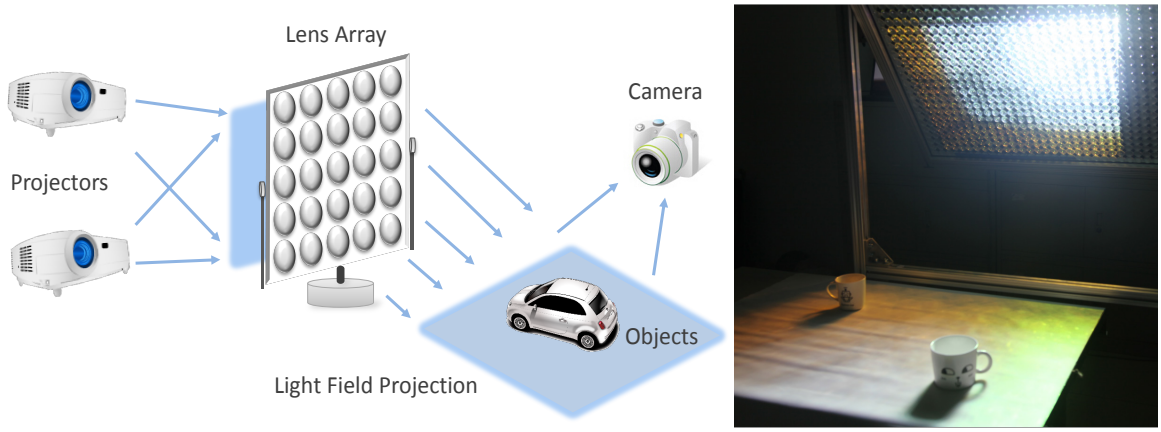

Figure 1: Overview of the light field projection system. (Left) A conceptual diagram of the system. The lens array focuses the projected light to produce a controllable light field for real objects lighting. A camera is used to capture the lighting result directly. (Right) One scene of the light field projection. Two cups are illuminated by the projected light field.

ABSTRACT

We propose a novel approach to generate 4D light field in the physical world for lighting reproduction. The light field is generated by projecting lighting images on a lens array. The lens array turns the projected images into a controlled anisotropic point light source array which can simulate the light field of a real scene. In terms of acquisition, we capture an array of light probe images from a real scene, based on which an incident light field is generated. The lens array and the projectors are geometric and photometrically calibrated, and an efficient resampling algorithm is developed to turn the incident light field into the images projected onto the lens array. The reproduced illumination, which allows per-ray lighting control, can produce realistic lighting result on real objects, avoiding the complex process of geometric and material modeling. We demonstrate the effectiveness of our approach with a prototype setup.

Keywords: Light field projection, virtual reality, lighting reproduction, realistic lighting, matting and compositing.

Index Terms: B.4.2 [Input/Output and Data Communications]: Input/Output Devices—Image display; I.3.7 [Computer Graphics]: Three-Dimensional Graphics and Realism—Virtual reality

1 INTRODUCTION

Many applications of virtual reality involve lighting control that adjusts intensity and color of spatial light. An important application of lighting control is to reproduce the lighting environment of a scene in another scene. The lighting reproduction provides consistent illumination in different scenes, which was employed in previous researches of user immersion [1], compositing [2], and augmented reality [3, 4]. However, most of the existing work just provides a coarse lighting control which leads to an inaccurate lighting reproduction. We present an approach of light field projection based on multi-projector and lens array that could provide accurate per-ray lighting control. Figure 1 illustrates the conceptual diagram and shows a prototype of the light field projection approach. A projected light field is generated via multi-projection on the lens array screen. Real objects are illuminated by the projected light field would appear to be the same as they were in the original lighting environment.

The proposed light field projection aims at generating an accurate lighting environment that could be used for realistic lighting on real objects. In computer graphics, simulating lighting on real objects require complex geometric modelling and reflectance measuring that are both tedious and computational expensive [5, 6, 7]. The main motivation of the proposed light field projection approach is to accurately reproduce the illumination and get the lighting result of real objects without any geometric and reflectance modeling or computation.

The main contribution of this paper is a novel approach of light field projection that can generate 4D light field in physical world based on lens array and projectors. The lens array turns the projected images into an anisotropic point light source array with a customized optical design, which provides a flexible scheme to simulate the light field of a real scene. Compared to previous approaches such the lighting stage [2], our system is inexpensive, simpler to setup and enable much finer control of the simulated lighting environment.

From a system perspective, we adopted multi-projector display techniques to increase the field of view and resolution of the projected light field. In addition, we developed techniques to acquire real-world incident light field and synthesize the images to be projected given a multi-projector/lens array setup. A

† zz@buaa.edu.cn
*yutao12@gmail.com

IEEE Virtual Reality Conference 2015
23 - 27 March, Arles, France
978-1-4799-1727-3/15/$31.00 ©2015 IEEE

prototype is constructed to demonstrate the effectiveness of our approach.

2 Related Work

Our work is closely related to three areas: lighting reproduction, light field system, and projection calibration. This section reviews the related progresses in the three areas.

2.1 Lighting reproduction

Lighting consistency plays an important role in many virtual reality applications. An effective way is lighting reproduction, which refers to the creation of a lighting environment that is as close as to the scene being reproduced. Lighting reproduction has been explored in some prior work. Debevec et al. [2] built a light stage with 156 RGB LED lights toward the center of the stage. These LED lights were driven by an environment map so as to reproduce the illumination of the environment. The reproduced light illuminated an actor who was then composited into the environment with same illuminating. This work demonstrated a great lighting consistency in composite image, and it had actually been employed in film making. However, three limitations exist due to its structure. Firstly, only the illumination of the light stage center can be reproduced, so it is usually just used to illuminate the actor's face. Secondly, the light stage just provides a directional-only illumination, lacking fine-grain spatial variation. Finally, the accuracy of the reproduced lighting depends on the amount of the LED lights, which is hard to scale. In our work, the light field projection approach achieves an accurate and spatial varying lighting reproduction.

Some researches on augmented reality employ lighting reproduction for creating a sense of immersion. Ghosh et al. [1] introduced a lighting control method for reproducing illumination of a virtual world in a room. They used 24 RGB LED lights that are distributed throughout the room to reproduce the illumination approximating an environment map for the assumed viewing position. Noh et al. [3] proposed an augmented reality system that enable user to interactive control of the illumination distribution in a real room using a computer-controlled lights array. Cutler's group [4,8] presented an approach of spatially augmented reality for architectural daylighting design by projecting rendered images as direct illumination to a real model. The existing work used LED lights or small number of projectors as light source that resulted in a low-resolution illumination. In contrast, we employ a multi-projector and lens array based approach to generate an accurate lighting with high spatial resolution.

2.2 Light Field System

Light field has been well studied. Levoy and Hanrahan [9] introduced the 4D light field representation *light slab* into computer graphics, which is the data representation of most light field research. Unger et al. [10] presented a process for capturing incident light field with translation stage or mirror sphere array. Microlens array or spatial light modulator were used for light field photography [11, 12], but the spatial sampling of the light field is rather narrow in directions. Masselus et al. [7] reconstructed a 4D incident light field for relighting by moving a single projector around the scene. However, the 4D relighting usually requires heavy computation [6, 13].

Light field display is a technique closely related to our work in optical structure. Steele and Jaynes [14] constructed a prototype of light field display using a 5×4 array of projectors, and they also suggested that a lens array would be necessary for greater spatial resolution. Multiple projectors and a microlens array were used to simulate a light field for autostereoscopic display in some solutions [15, 16]. Array of projectors and cameras were also used to create 3D TV system [17, 18] by integral photography and multi-projection on lenticular screen. Jurik et al. [19] presented a full-parallax light field display by direct observation of an array of pico-projector. Matthew et al. [20] presented a compressive light field projection system that comprised a customized light field projector and an angle-expanding screen for glasses-free 3D display. Two high-speed spatial light modulators are used to generate light field and two lenticular sheets are mounted back-to-back to expand the field of view. However, the number of views is limited. The other work mentioned above shared a similar drawback that they were uneasy to allocate spatial or angular resolution. In our work, a flexible resolution control is achieved owing to a customized optical design.

The work most similar to ours is the light field transfer by Cossairt et al. [21] to composite real and synthetic objects in one scene. Indirect lighting was transferred between real and synthetic objects via a light field interface. The illumination part of the setup in this work does similar to the proposed light field projection. Though, there are some different contributions in our approach contrast to this work. Firstly, the illumination acquisition and projection of the light field transfer are through one lens array which causes a narrow and low-resolution view. Consequently extra light source and dark background are essential for the light field transfer system while it is unnecessary in our work owing to the panorama capturing and wider projection field. Secondly, we de-couple the capture and synthesis process, which makes it more flexible. Our approach also better fits for dynamic scenes because the capturing and computation processes are pre-processed and the illumination stage could be real-time. Thirdly, our approach provides a more general way to synthetic image composition with background environment as exceeds the scope of the light field transfer.

2.3 Projection Calibration

The calibration of multi-projection mainly involves geometric and photometric calibration. The geometric calibration technique can be divided into two categories based on the display surface, planar or non-planar. As our work is based on planar display surface, we only introduce related work in this sub-area. The key of registering projected image on a planar display surface is establishing of 2D homography between the two [22]. Most prior work projected known features to compute the homographies [23, 24]. We adopted this method to calculate the homography by using a camera which is also used in photometric calibration.

Due to the reason of projector lamp age, type, position, etc. the photometric variation of projection can be significant, even with same input. Majumder and Stevens [25] proposed that the main cause of the photometric variation was luminance since the luminance of projectors showed large spatial variation while the chrominance was almost constant spatially. Thus an *intensity transfer function* (ITF) which defines the intensity transfer ratio of a single channel of a projector can be used to measure the photometric variation. Raij et al. [26] evaluated the ITF by adopting high dynamic range (HDR) imaging method using a black and white camera. We employ the HDR imaging method to measure ITF for color correcting, and dynamic range mapping is done to meet the requirement of reproducing HDR illumination.

3 Light Field Projection

This section describes the process of light field projection. Firstly, we describe its optical design. Secondly, we present an incident light field generation approach using the light data captured in a real scene. Thirdly, to recover the incident light field, sub-images for each lens are synthesized and composited into the final projection image.

3.1 Optical Design

The major goal of the optical design is to create a controllable light field in physical world. To achieve this, we propose a light field projection system that consists of multi-projector and a lens array. Figure 2 illustrates the generation of the projected light field. Projectors project images onto the lens array, and the lens array focuses these light rays at some points which are the image points of the projector apertures. These focused points constitute an array of point light source. The light rays continue to spread from these points are from the projected images which can be easily controlled. Therefore, a controlled anisotropic point light source array is generated that each point can be seen as a sub-projector. These sub-projectors form a projected light field.

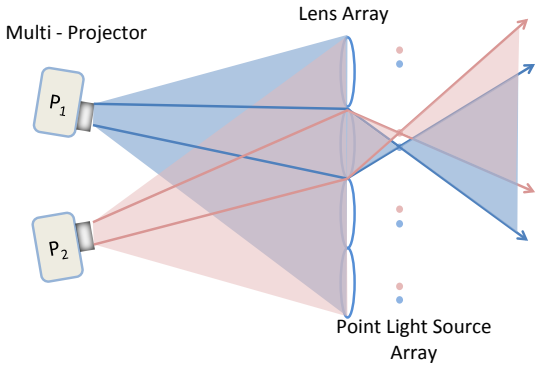

Figure 2: Multi-projector project images onto the lens array by which the projected light rays are focused at a point light source array. This point array constitutes a light field in physical world.

Resolution: Each lens generates an image point for each projector, so the spatial resolution of the projected light field is:

$$R_{spatial} = n_P \times n_L \tag{1}$$

where $R_{spatial}$ is the spatial resolution, n_P is the number of projectors, and n_L is the number of lens. The angular resolution is defined as the amount of light rays each point light source can emit, it is given by:

$$R_{angular} = \frac{R_P}{n_L} \tag{2}$$

where $R_{angular}$ is the angular resolution, and R_P is the resolution of projectors.

The existing work based on projectors only [14, 19], provide a high angular resolution (projector resolution), and low spatial resolution (projector number). Conversely, the microlens screen based solutions [16, 17, 20], provide a high spatial resolution (microlens screen resolution), and low angular resolution. Neither solutions mentioned above is desirable for lighting reproduction, because low spatial resolution causes a discontinuous light source distribution or a small light source area, and low angular resolution causes a narrow field of view or a shallow depth of field. By contrast, our optical design has a flexible configuration on both spatial and angular resolution. Each additional projector increases the spatial resolution by the resolution of lens array. Meanwhile, we can increase the angular resolution by using high resolution projectors or using fewer lenses on the lens screen with the same projector resolution.

Field of View: We use a lens array in which each lens is with 40mm focal length and 25mm diameter for the projection screen. It generates a maximal angle about 35°of the field of view in a single point light source. By adjusting the relative position and orientation of the multi-projector and lens screen, a wider field of view can be achieved in the whole screen area.

Depth of Field: Commercial projectors have a limited depth of field. To solve this problem, we employ a secondary imagery method to extend the depth of field for the projected light field. Figure 3 is a 2D schematic diagram illustrating the light path of a single pixel through a lens. As shown, the focal plane of projection is adjusted to the place between *f* plane (focus plane of lens) and *2f* plane. As *f* (focus of lens) is small, 40mm in our prototype, the depth of field of the projector can cover most scope between *f* plane and *2f* plane, even all the scope. Consequently, we can easily infer from geometrical optics that the depth of field in secondary imagery through a lens will cover from *2f* plane to infinite far, in theory, until attenuating to be undetectable.

As illustrated in Figure 3, the light from a red pixel in the projector are focused at the projection image, and refocused by a lens via the image point of the projector aperture to secondary imagery plane, then spreading. Owing to the deep depth of field in secondary imagery area, the light can be seen as an ideal light ray from a point light source. All the light emitted from the projector and through the lens form an anisotropic point light source. All the projectors and lens array create an anisotropic point light source array. That is projected light field generated.

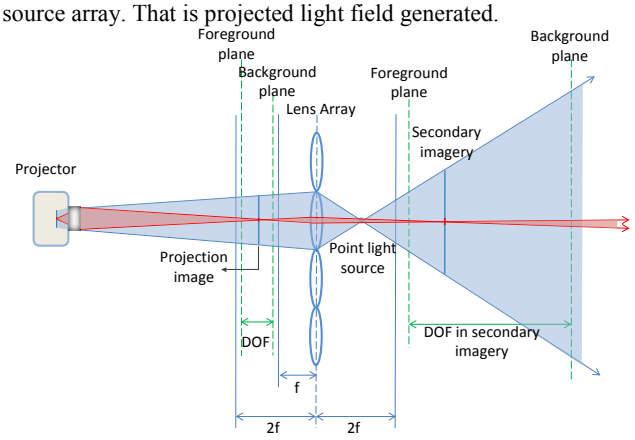

Figure 3: The illustration of secondary imagery. The projector projects an image at the position between *f* plane and *2f* plane. The depth of field of the projector covers most scope between *f* and *2f* plane. After a secondary imagery via a lens, the depth of field in secondary imagery area extends to from *2f* to infinite.

3.2 Incident Light Field Generation

For lighting reproduction of a scene, we should model the lighting of the scene at first. A 4D incident light field generation approach based on light probe array is presented. It shares the same representation with the projected light field so that it can be easily converted.

Firstly, we acquire the illumination data in a scene via light probe array that captured by a 2D translation stage and a panorama camera [10]. The translation stage is driven by digital control with sub-millimeter accuracy in position. Several panoramas with different exposures are captured at each location to assemble a HDR light probe. The illumination capturing is carried out in the motion range of the translation stage, and it is fully-automatic. The captured result is a light probe array recording the incident light in the range.

Then we can generate an incident light field based on the captured light probes. Since the projectors and lens array are fixed

and geometric calibrated in advance, the image plane of the projector apertures is determined, as the *uv* plane in Figure 4. The light probes are captured on the translation stage plane and moved to the place we reproduce the illumination, as the *st* plane in Figure 4. Then, a 4D incident light field is generated in a two-plane based representation, similar as the *light slab* [9]. The representation is:

$$L_{(u,v,s,t)} \rightarrow RGB \tag{3}$$

where *(u, v)* and *(s, t)* are the plane coordinates. *L(u, v, s, t)* refers to the intensity of the corresponding light ray sample, it is given by the value of the intersecting pixel on the light probe.

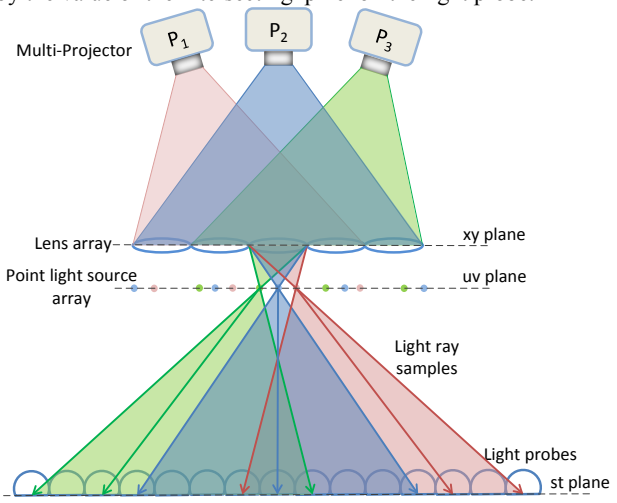

Figure 4: Projectors project images onto lens array, and generate a point light sources array as projected light field. Captured light probes are used to generate a 4D incident light field in the same structure of the projected light field with the representation of *(u,v,s,t)*.The incident light field is reproduced by the projected light field to implement the lighting reproduction.

3.3 Projected Image Synthesis

After the incident light field is generated, we recover it from the projected light field for lighting reproduction. The projected light field is generated by multi-projection on the lens array, and it is in the representation of anisotropic point light source array which can also be seen as a sub-projector array. Hence, the producing of the projected light field is disintegrated as image synthesizing of each sub-projector and image stitching for final projection of each projector.

Sub-Projector Image Synthesis: As shown in Figure 4, the sub-projectors locate in the *uv* plane. Their positions are calculated by the relative position of the projectors and the lens array. Then, the cover range on *st* plane of the emergent light of each sub-projector can be solved by intersecting light rays from the corresponding sub-projector and lens.

For each sub-projector in *uv*, a synthetic *st* image is required. As illustrated in Figure 5, the cover range on *st* plane of each sub-projector is indexed by its position *(u, v)*. The light ray samples of each sub-projector intersect with the corresponding light probes at one pixel. Assembling these pixels according to their position, a rough *st* image is generated. The resolution of the *st* image is the angular resolution of the projected light field. Generally, it too sparse for projection, unless an extremely dense sampling of light probes is made. So, up-sampling for these *st* images are necessary.

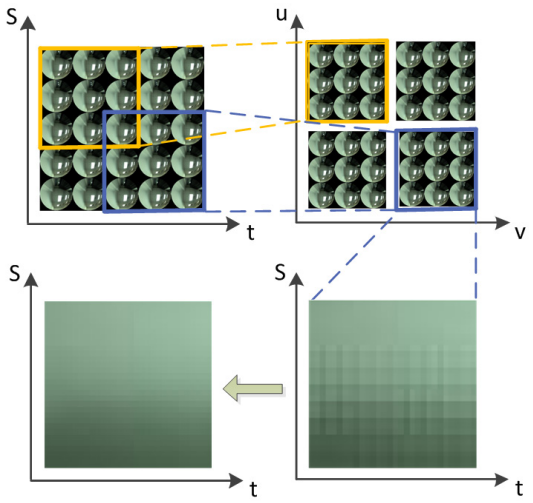

Figure 5: The process of synthetizing the sub-projector image. (Top) The light probes in the cover range of each sub-projector are picked out and indexed by the position of the sub-projector. (Bottom) One pixel from each light probe, which is the intersection pixel of the light ray samples, forms a synthetic image. An interpolation to increase the image resolution is implemented for projection.

Radial Distortion Correction: As fish eye lenses are used to make the lens screen for wide field of view, an obvious radial distortion arises in secondary imagery. Thus, the synthetic sub-projector images need a radial distortion correction. We employ the single parameter division distortion model [27] to estimate the radial distortion as it better suits fish eye lens than others.

The projected image of a projector on the lens screen can be disintegrated as pieces that each piece just covers a single lens. Each piece image is synthetized by distortion correcting of the corresponding sub-projector image.

Integrated Image Stitching: After all the pieces of these sub-images from a projector are generated, the required projection image of the projector is directly spliced by these sub-images. Figure 6 shows a light probe sample of an outdoor scene and the corresponding integrated projection image of the scene. Restricted by the field of view of the projected light field, the recovered illumination of the scene is mainly from sky. More projectors and more lens array sets may produce a more intact scene illumination.

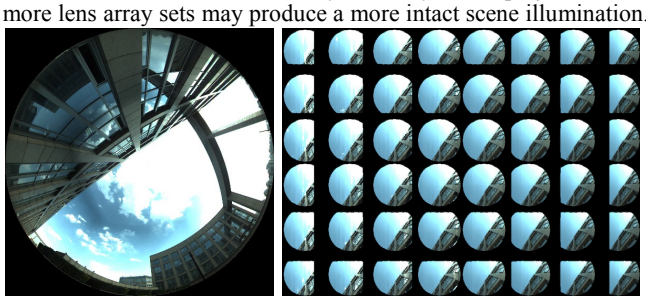

Figure 6: The integrated image stitching for the projected light field generation of an outdoor scene. (Left) A light probe sample of the scene. (Right) The projection image that spliced by sub-images.

4 System Calibration

This section presents the procedures to calibrate the geometry relation between the input image of projectors and the lens array. And the photometric calibration for color consistency and dynamic range mapping of the projected images is shown.

4.1 Geometric Calibration

The purpose of geometric calibration is to generate a point-to-point correspondence between the input image and the lens screen surface for each projector to align the projected light field. This correspondence is defined as a 3×3 homography matrix that can be established with only four known point correspondences. The homography is solved by a homography concatenation via a camera [23]. It is given by:

$$H_{lp} = H_{cp} H_{lc} \tag{4}$$

where H_{lp} is the homography from the lens array to a projector, H_{cp} is the homography from the camera to the projector, and H_{lc} is the homography form the lens array to the camera. The H_{lp} is directly got by a homography transfer of H_{cp} and H_{lc}, thus they are computed instead.

The lenses of the lens screen used in our prototype are plano-convex, and glued on a glass pane. For geometric calibration, we place a white curtain on the back of the glass pane as the display surface of projection. A picture of the surface is taken using the camera. The four corners of the white curtain are directly used as feature points to compute H_{lc}. The H_{cp} is unique for each projector so that it needs to be computed respectively. The process of computing H_{cp} is similar with that of H_{lc} by projecting features on the white curtain and establishing a correspondence of the features and their image. We employ the method presented by Raskar et al. [24] to compute the H_{cp} via projecting a checkerboard on the white curtain and find its corner automatically. As more than four point correspondences are found, the least-squares solution is adopted for H_{cp} computation.

After the H_{lc} and H_{cp} are both solved, the H_{lp} for the corresponding projector is directly concatenated by the two. Then, the input image of the projector is able to be generated from the integrated image via the H_{lp}.

4.2 Photometric Calibration

The reproduced light is captured by a camera and generated from projectors. An obvious chromatic aberration may arise if the pixels of the captured light probes are directly used as the input of the projectors. Another problem is that the dynamic range of a scene is much higher than that of projectors can provide. The photometric calibration is performed for achieving color uniformity for multi-projection and making the dynamic range of the reproduced illumination match the captured scene.

Color Uniformity: As proposed in some previous work [22, 25], the spatial variation in luminance is the most significant cause of the color variation in multi-projection, while the chrominance is almost spatially uniform so that the variation in chrominance can be ignored. Besides, the sensitivity of human to luminance variation is at least an order of magnitude higher than to chrominance variation. So we simplify the color calibration to luminance calibration for all projectors.

The luminance calibration is processed separately for RGB channels. It is implemented by computing the *intensity transfer function* (ITF) which is defined as the luminance transfer ratio form the input of pixel value. The ITF is given by:

$$r_c(x, y, i_c) = \frac{L_c(x, y, i_c) - B(x, y)}{W_c(x, y) - B(x, y)} \tag{5}$$

where c is a given channel from RGB, (x, y) is the position coordinates of the lens screen surface, $W_c(x, y)$ is the maximum luminance projected to (x, y) with the input 255 at channel c and 0 at the other two channels, and $B(x, y)$ is the minimum luminance projected to (x, y) with the input (0, 0, 0). $B(x, y)$ would not to be totally black as the black offset exists when projecting. $W_c(x, y)$-$B(x, y)$ defines the luminance range that the projector can provide from channel c. i_c is the input of channel c for a given pixel, $L_c(x, y, i_c)$ is the output luminance projected to (x, y) with the input i_c. The transfer ratio $r_c(x, y, i_c)$ defines the output proportion of the luminance with the input i_c at (x, y). Raij et al. [26] have shown that the ITF is spatially invariant across the whole projection surface, so the transfer ratio $r_c(x, y, i_c)$ is able to be simplified as $r_c(i_c)$. The computation of the ITF is actually establishing the relation between the input i_c and the output ratio r_c.

We employ the HDR imaging technique to compute the ITF for each projector [26]. The same camera used in geometric calibration is also used for HDR imaging to the projection surface with various projection input. HDR images are evaluated for input from black (0) to white (255). Each HDR image represents a discrete measurement of the luminance across the whole projection surface. As the ITF is spatial invariant, a small set of pixels at the center of the projection surface in the HDR images are averaged to compute the luminance and the transfer ratio. 27 discrete transfer ratios with interval of every 10 input values are measured and fitted as the ITF of a given channel. RGB ITFs are measured respectively. After the ITFs are drawn, for projecting a given intensity L_c at (x, y), it is first to compute the transfer ratio r_c according to the equation 5. Then, the corresponding input i_c is directly got from the ITF.

Dynamic Range Mapping: In general, the dynamic range of a scene is much higher than the projecting light. We capture the illumination via HDR light probes that needed to be mapped to the input of projectors with a reduction of the dynamic range. The linear compression for the dynamic range is physically correct, but it just keeps the contrast in medium area while causes a detail loss in bright and dark areas. Inspired by the tone mapping technique, we employ a nonlinear compression method based on the logarithmic compression of luminance values, imitating the human response to light. This logarithmic compression is executed for each RGB channel and it is written as:

$$R_c(x, y) = \frac{\log_b(P_c(x, y) + 1)}{\log_b(P_{cMax} + 1)} \tag{6}$$

where for a given projector and given channel c, $P_c(x, y)$ is the pixel value of channel c at the position (x, y) of the integrated image on the lens screen surface, and P_{cMax} is the maximum value among the $P_c(x, y)$. From the equation, the mapping ration $R_c(x, y)$ falls in the range of 0 to 1.0. The value of logarithmic base b has a great impact to the mapping ratio in dark and bright areas. Drago et al. [28] propose that an adaptive adjustment of the base according to each pixel value can provide good contrast and detail preservation in dark and bright areas. We follow this method to compute $R_c(x, y)$ with a varying base b.

After the mapping ratio $R_c(x, y)$ of each channel and each pixel are solved, the required output luminance $L_c(x, y)$ of the corresponding projector is given by:

$$L_c(x, y) = B_{Max} + R_c(x, y) \cdot (W_{cMin} - B_{Max}) \tag{7}$$

where for all the projectors, B_{Max} is maximum luminance value of the black offset (brightest black pixel), and the W_{cMin} is minimum luminance value with maximum input in channel c (darkest white pixel in channel c). Thus, the range from B_{Max} to W_{cMin} is the

common luminance range that each projected pixel can arrive. Then the required output luminance $L_c(x, y)$ is linear mapped to the range based on the corresponding mapping ratio $R_c(x, y)$. With the known output luminance, the pixel values of the input image for each projector are got from the equation 5 and the ITF curve.

5 Implementation

We build a prototype for presenting light field projection. This section describes the implementation of the prototype.

5.1 Hardware

Our prototype is comprised of two projectors and a lens array screen for lighting reproduction. A panorama camera and a translation stage are used for illumination capture of real scenes.

Illumination Capture: We place a panorama camera on a 2D translation stage to capture light probes. The panorama camera we used is Ladybug3 from Point Grey. It contains six 2 megapixels cameras that enable us to capture 12 megapixels fused panoramas at 15 fps. The translation stage is driven by a numerical control device with sub-millimeters accuracy in movement. It contains two axles crossing vertically, and each of the axles is 50cm long with a shortest step of 2mm. We employ a uniform capturing strategy with 50×50 sampling locations in the moving range of the translation stage. To composite HDR light probes, 8 panoramas with different exposures are captured at each sampling location. The whole capturing procedure takes approximately 3 hours.

Multi-Projection: The light field projection is implemented by multi-projection on a lens array. Two off-the-shelf projectors Sony VPL-FX41 and Hitachi HCP-900X are used, and both of them have a standard resolution of XGA. The lens array screen is 1m×1m with 36×36 plano-convex lens glued on it, and it can be rotated around its center axis. Each lens has same optical parameters that are 40mm focal length and 25mm diameter. The rhombic gaps in-between the lenses are blocked up to stop the light from crossing here, while the light through the lenses are focused as projected light field. The camera Flea2 from Point Grey is used for the calibration of the multi-projection.

5.2 Software

Every 8 panoramas captured at a same sampling location are exposed from 0.25ms to 32ms in approximately 1-stop increments to composite a HDR light probe. We use HDR Shop [29] to implement the composition. In the computation of ITFs, the images of the projection surface also require HDR compositing. One HDR image is composited for every input of projectors from 0 to 255 with interval of 10 yielding 27 HDR images for each channel of each projector. Every HDR image is created from 15 exposures ranging from 0.0625ms to 500ms.

After the light field projection is achieved, we implement a matte extraction. It is implemented by applying the GrabCut algorithm [30] in OpenCV. The matte is used to extract objects from the reproduced illumination.

6 Results

To investigate a detailed lighting reproduction, we construct a test scene with characteristic illumination. As shown in Figure 7(a), 5 color LED spotlights are placed toward a plane on which 5 color circles are generated. We capture light probes on the plane to record the characteristic illumination. Figure 7(b) is a light probe sample of the test scene and Figure 7(c) is a photo of the plane.

The reproduction result of the test scene is shown in Figure 8. Figure 8(b) is a synthesized input image for the projection and Figure 8(a) is a photo of the reproducing scene in our prototype. Figure 8(c) shows the final result of lighting reproduction of the test scene. Due to the overexposure of the LED lights, the center

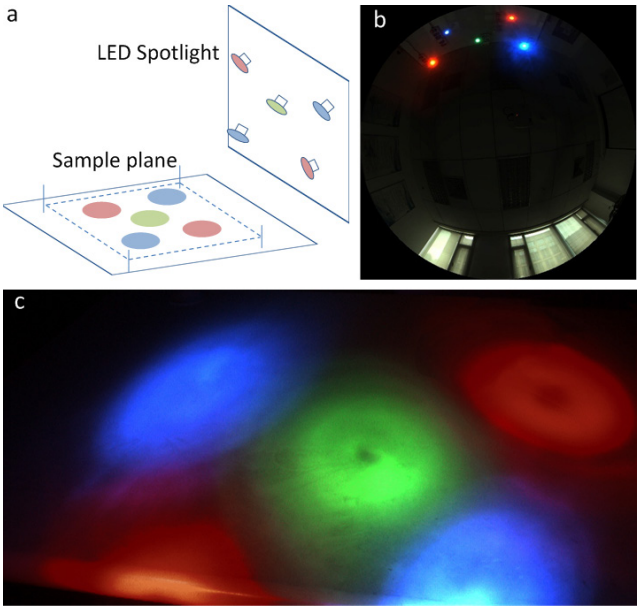

Figure 7: A test scene with characteristic illumination. (a) The sketch of the test scene. 5 color LED spotlight are pointed at a plane. (b) A light probe sample of the test scene. (c) The real photo of the sample plane.

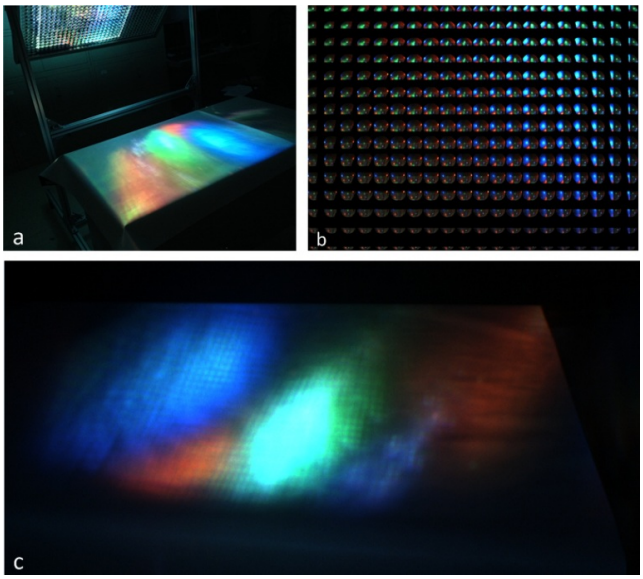

Figure 8: The result of the illumination reproduction of the test scene. (a) The reproduction in our prototype. (b) A sample of the synthesized input images of the projectors. (c) The final result of the reproduced illumination that generated by the light field projection.

of the lights becomes white and halos arise in the light probe images which result in an imperfect reproduction in Figure 8(c). Consequently, the shapes of the color circles are not exactly the same and the center become white as well. Though, the color and distribution of the illumination area are exactly reproduced. The grid effect in Figure 8(c) is caused by the magnification of the lens array to the projector pixels. Insertion of diffusers may eliminate the effect, but it will decrease the angular resolution. Compared with the prior solutions, the proposed light field projection achieves a light field reproduction in real scene.

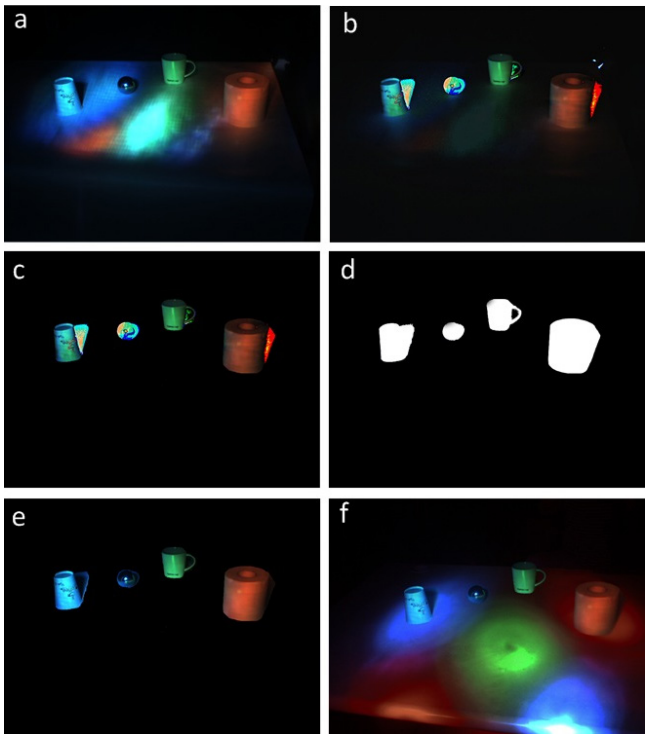

Figure 9: The process of objects matting and composite. **(a)** The image of some objects illuminated by the reproduced illumination. **(b)** The difference image of subtracting 10(c) from 11(a). **(c)** GrabCut result for clean matte extraction. **(d)** The mask of these objects generated from (c). **(e)** The objects are extracted from (a) with the mask (d). **(f)** The final compositing result.

We demonstrate a matte extraction of real objects from the reproduced illumination, and composite them into the background environment with consistent illumination. The process is illustrated in Figure 9. Figure 8(c) shows the reproduced lighting environment. Figure 9(a) is an image of some objects illuminated by the reproduced illumination. 9(b) is the difference between 9(a) and 8(c). However, the matte is not clean enough for objects extraction. We apply the GrabCut algorithm [30] for a clean matte extraction, the result is shown in 9(c). And a binarized mask is directly obtained in 9(d). Then, these objects are re-extracted form 9(a), resulting the only extracted objects and shadows in 9(e). Finally, these extracted objects and shadows are composited into the corresponding background environment, as is shown in 9(f). The compositing result shows a consistent lighting effect.

Figure 10 demonstrates a compositing in a virtual scene. It is a desk of wood texture with highlights on it. Figure 10(a) is the rendering image of the virtual scene. We capture the illumination of the virtual scene by using virtual camera array in the model, and reproduce the illumination in the physical world to illuminate two cups, as is shown in Figure 10(b). Figure 10 (c) shows the composite of the two cups and other three synthetic objects. The two cups are placed at the center and edge of the highlighted area respectively. They show an appropriate lighting effect and generate a realistic sense of immersion in the composite image.

Figure 11 demonstrates another composite image to show the caustics which can be easily generated by our approach. Some complicated lighting effects require amount of computation in conventional 3D rendering, such as the caustics. These effects can be directly obtained in the light field projection, and show a more realistic lighting than rendering. It is a simple and efficient way to get these complicated lighting effect contrast to rendering.

Figure 10: The composition of real objects in virtual scene. (a) The virtual scene with a highlighted area. (b) Two cups are illuminated by the illumination of the virtual scene. (c) The two cups and three virtual objects are composited into the virtual scene.

Figure 11: A composite of two cups of tea to show the caustics. (Left) The illuminated result. (Right) The composite image.

7 Discussion

In this section, we discuss the benefits and limitations of the proposed light field projection approach and the directions for future research.

7.1 Benefits and Limitations

Among the existing work on lighting reproduction or illumination control, LED lights or conventional projectors are used as the light sources. Though they provide a sense of immersion, the lighting is rough as the low resolution of the light sources. In contrast, the proposed light field projection approach achieves a per-ray level lighting reproduction by generating a 4D light field in the physical world. And a flexible resolution control is implemented in our approach. The principle of the light field display and autostereoscopic display is similar with our approach. However, for viewing purpose, they commonly take some steps to enhance the spatial resolution by lowering the angular resolution as a tradeoff. It is not desirable for complicated illumination. We solve this problem via a customized optical design for resolution allocation. Besides, most current approaches have a limitation of depth of field. We present a method of extension of the depth of field via secondary imagery of the lens array. It can be also applied in any projection-based display system. For applications, the light field projection provides an alternative way of 3D rendering for real objects illumination. It is efficient and requires no geometric and material information. It can be used in studio shot with exterior illumination.

Since the limited field of view of our prototype, we place the predominant light source inside the angular range of the lens array. A new prototype with three lens array and more projectors is planned to be built for a more intact illumination generation. Compared with the real scene, the resolution, luminance and dynamic range of the projectors are limited. It is an inherent problem resulted from the existing commercial projectors. The rapid development on pico-projector and micro-projector production may solve the problem in a short future. Another limitation of our prototype is the basic assumption of 4D light field that the radiance of light rays along their path does not attenuate in the 4D light field. It does not fit the reality of lighting in a large scene. Yet, it can be solved by a 5D light field reproduction which is the major direction of our future work.

7.2 Future Work

Our prototype employs a 4D light field model that it assumes the radiance of the light rays keep consistent in their spread. Actually a varying attenuation exists according to the propagation distance of each light ray. Thus the attenuation calibration is a direction of the future work, which means a 5D light field reproduction. A spatially varying light field reproduction is implemented in our prototype, and time-varying lighting reproduction can also be attained based on time-varying incident light field acquisition.

8 Conclusion

We propose a novel approach of light field projection for accurate lighting reproduction. A 4D light field with flexible resolution control and deep depth of field is generated in real scene by multi-projection on a lens array. The projected light field is used to reproduce the illumination that captured in another scene. The reproduced illumination can be used for realistic lighting on real objects instead of rendering. Beyond the lighting reproduction, complex lighting customizations for various applications can also be performed through the light field projection approach. It is our hope that the light field projection will bring some novel ideas in lighting reproduction, and inspire others in any aspects.

Acknowledgments

This paper was supported by the National High Technology Research and Development 863 Program of China under Grant (No. 2012AA011801 and No. 2012AA011803) and National Natural Science Foundation of China (No. 61472020).

References

[1] A. Ghosh, M. Trentacoste, H. Seetzen, & W. Heidrich. Real Illumination from Virtual Environments. In Eurographics Symposium on Rendering. Eurographics Association, 243-252, 2005.

[2] P. Debevec, A. Wenger, C. Tchou, A. Gardner, J. Waese, & T. Hawkins. A lighting reproduction approach to live-action compositing. ACM, 21(3):547-556, 2002.

[3] S. T. Noh, S. Hashimoto, D. Yamanaka, Y. Kamiyama, M. Inami, & T. Igarashi. Lighty: A painting interface for room illumination by robotic light array. In Mixed and Augmented Reality (ISMAR). IEEE, 305-306, 2012.

[4] Y. Sheng, T. C. Yapo, C. Young, & B. Cutler. A spatially augmented reality sketching interface for architectural daylighting design. Visualization and Computer Graphics, IEEE Transactions on, 17(1):38-50, 2011.

[5] A. Wenger, A. Gardner, C. Tchou, J. Unger, T. Hawkins, & P. Debevec. Performance relighting and reflectance transformation with time-multiplexed illumination. In ACM Transactions on Graphics (TOG), 24(3):756-764, 2005.

[6] A. Jones, A. Gardner, M. Bolas, I. McDowall, & P. Debevec. Simulating Spatially Varying Lighting on a Live Performance. Conference on Visual Media Production (CVMP), 2006.

[7] V. Masselus, P. Peers, P. Dutr, and Y. D. Willems. Relighting with 4d incident light fields. ACM Trans. Graph, 22(3):613–620, 2003.

[8] J. Nasman, B. Cutler. Evaluation of user interaction with daylighting simulation in a tangible user interface. Automation in Construction, 36: 117-127, 2013.

[9] M. Levoy, & P. Hanrahan. Light field rendering. In Proceedings of the 23rd annual conference on Computer graphics and interactive techniques. ACM, 31-42, 1996.

[10] J. Unger, A. Wenger, T. Hawkins, A. Gardner, & P. Debevec. Capturing and Rendering with Incident Light Fields. In EGSR, 2003.

[11] R. Ng, M. Levoy, M. Brédif, G. Duval, M. Horowitz, & P. Hanrahan. Light field photography with a hand-held plenoptic camera. Computer Science Technical Report (CSTR), 2(11), 2005.

[12] K. Marwah, G. Wetzstein, Y. Bando & R. Raskar. Compressive light field photography using overcomplete dictionaries and optimized projections. ACM Transactions on Graphics (TOG), 32(4):46, 2013.

[13] P. Sen, B. Chen, G. Garg, S. R. Marschner, M. Horowitz, M. Levoy, and H. P. A. Lensch. Dual photography. ACM Transactions on Graphics, 24(3):745–755, 2005.

[14] M. Steele & C. Jaynes. Interactive light field display from a cluster of projectors. In ACM SIGGRAPH 2003 Sketches & Applications, 1-1, 2003.

[15] H. Sakai, M. Yamasaki, T. Koike, M. Oikawa, & M. Kobayashi. 41.2: Autostereoscopic display based on enhanced integral photography using overlaid multiple projectors. In SID symposium digest of technical papers, 40(1):611-614, 2009.

[16] R. Yang, X. Huang, S. Li & C. Jaynes. Toward the light field display: Autostereoscopic rendering via a cluster of projectors. Visualization and Computer Graphics, Transactions on, 14(1):84-96, 2008.

[17] W. Matusik, & H. Pfister. 3D TV: a scalable system for real-time acquisition, transmission, and autostereoscopic display of dynamic scenes. In ACM Transactions on Graphics (TOG), ACM, 23(3):814-824, 2004.

[18] Y. Taguchi, T. Koike, K. Takahashi, & T. Naemura. TransCAIP: A live 3D TV system using a camera array and an integral photography display with interactive control of viewing parameters. Visualization and Computer Graphics, IEEE Transactions on, 15(5):841-852, 2009.

[19] J. Jurik, A. Jones, M. Bolas, & P. Debevec. Prototyping a light field display involving direct observation of a video projector array. In Computer Vision and Pattern Recognition Workshops (CVPRW), IEEE Computer Society Conference on, IEEE, 15-20, 2011.

[20] M. Hirsch, G. Wetzstein, R. A. Raskar. A compressive light field projection system. ACM Transactions on Graphics (TOG), 33(4):58, 2014.

[21] O. Cossairt, S. K. Nayar, R. Ramamoorthi. Light field transfer: global illumination between real and synthetic objects. ACM Transactions on Graphics (TOG), 27(3), 2008.

[22] M. Brown, A. Majumder, & R. Yang. Camera-based calibration techniques for seamless multiprojector displays. Visualization and Computer Graphics, IEEE Transactions on, 11(2):193-206, 2005.

[23] H. Chen, R. Sukthankar, G. Wallace, & K. Li. Scalable alignment of large-format multi-projector displays using camera homography trees. In Proceedings of the conference on Visualization'02, IEEE Computer Society, 339-346, 2002.

[24] R. Raskar, J. van Baar, & J. X. Chai. A low-cost projector mosaic with fast registration. In Asian Conference on Computer Vision (ACCV), 3(3), 2002.

[25] A. Majumder & R. Stevens. Color nonuniformity in projection-based displays: Analysis and solutions. Visualization and Computer Graphics, IEEE Transactions on, 10(2):177-188, 2004.

[26] A. Raij, G. Gill, A. Majumder, H. Towles, & H. Fuchs. Pixelflex2: A comprehensive, automatic, casually-aligned multi-projector display. In IEEE International Workshop on Projector-Camera Systems, 203-211, 2003.

[27] A. W. Fitzgibbon. Simultaneous linear estimation of multiple view geometry and lens distortion. In Computer Vision and Pattern Recognition (CVPR), 1:125-132, 2001.

[28] F. Drago, K. Myszkowski, T. Annen, & N. Chiba. Adaptive logarithmic mapping for displaying high contrast scenes. In Computer Graphics Forum, 22(3):419-426, 2003.

[29] P. Debevec & J. Malik. Recovering high dynamic range radiance maps from photographs. In ACM SIGGRAPH, 369–378, 1997.

[30] C. Rother, V. Kolmogorov, & A. Blake. Grabcut: Interactive foreground extraction using iterated graph cuts. In ACM Transactions on Graphics (TOG), 23(3):309-314, 2004.